Mixed Crystals of 6-Chloro-3,4-methylenedioxycinnamic Acid with 2,4- and 3,4-Dichlorocinnamic Acids; Structure, Topochemistry, and Intermolecular Interactions

Jagarlapudi A. R. P. Sarma and Gautam R. Desiraju *
School of Chemistry, University of Hyderabad, P.O. Central University, Hyderabad 500 134, India

The presence of a chloro substituent in a planar aromatic molecule tends to favour its crystallisation in the 4 Å short axis β-structure. This structure is stabilised by inter-stack Cl ••• Cl interactions which are weakly attractive yet directional in nature, and by intra-stack dispersive C ••• C interactions. The balance between intra- and inter-sheet interactions is revealed in the crystal structures of 6-chloro-3,4-methylenedioxycinnamic acid (**2a**), its 2:1 complex (**1a**) with 2,4-dichlorocinnamic acid, and its 1:1 complex (**1b**) with 3,4-dichlorocinnamic acid. The acid (**2a**) is dimorphic with both forms triclinic and with short axes *ca.* 4 Å; the structure of one form has been determined by *X*-ray diffraction methods. Solid-state u.v. irradiation of the complexes (**1a** and **b**) affords mixtures of mirror and pseudomirror symmetrical cyclobutanes; the formation of these products is consistent only with an ordered sheet-disordered stack structure, derived from the completely ordered structure of (**2a**), for these complexes. The structures of (**1a** and **b**) have been deduced thus on the basis of topochemical, kinetic, and crystallographic evidence, and provide important corroboration of inter-stack stabilisation as a prerequisite for β-structure adoption. Mixed crystalline complexes such as (**1a**) permit a comparative kinetic study of topochemical reactions, a procedure normally difficult in solid-state chemistry.

Ever since the pioneering work of Schmidt on the solid-state topochemical dimerisation of *trans*-cinnamic acids,[1,2] it has been realised that planar chloro-aromatic compounds (PCAs) tend to pack in modes characterised by a crystallographic short axis of *ca.* 4 Å (β-structure).[3–5] About a hundred β-structures of PCAs are reported in the 1984 version of the Cambridge Structural Database, and the structure is adopted by about forty other PCAs the cell dimensions of which were measured by Schmidt and his group.

There has been much discussion on the existence and nature of Cl ••• Cl non-bonded interactions in organic molecular crystals.[6,7] The most important characteristic of such interactions is that the distance between the two Cl atoms is less than twice the van der Waals radius. Whether Pauling's value for the Cl radius (1.80 Å) or more conservative values in the 1.75—1.80 Å range are used, a large number of Cl ••• Cl contacts in organic molecular crystals would have to be defined as short. Structural consequences of these short (3.2—3.6 Å) intermolecular Cl ••• Cl contacts are illustrated by crystal packings of the archetypal compounds 1,4-dichlorobenzene (triclinic form) and hexachlorobenzene. In the former, in-plane contacts of 3.38 Å are responsible for the formation of molecular sheets, which are then stacked at the van der Waals separation to optimise C ••• C contacts. In the latter, Cl ••• Cl contacts of 3.72 Å result in the molecules being arranged along linear ribbons which are stacked at the short axis separation. Successive stacks are related by two-fold screw axes and are held together by additional Cl ••• Cl contacts of 3.51 Å. The importance of Cl ••• Cl and C ••• C interactions in stabilising these simple β-structures has been discussed by us already.[8] To summarise, in these structures, molecular sheets or ribbons are stacked at van der Waals separation to generate the 4 Å short axis.

In this paper we describe the formation and solid-state chemistry of some β-structure molecular complexes which are held together by Cl ••• Cl, C ••• C, C–H ••• Cl and C–H ••• O interactions. A study of the packing characteristics of mixed crystals is a valuable approach towards understanding the nature of weak intermolecular interactions in organic solids, and a study of this type was undertaken to understand better the varying roles of intra-stack and inter-stack interactions in 4 Å β-structures.

The Importance of Molecular Complexes in Crystal Engineering.—While the stable crystal structure of most organic molecular solids is the result of a balance of a large number of relatively weak interactions, the formation of a molecular complex between two different compounds implies that it is possible to identify, dissect, and analyse a few significant interactions from this larger number.[9] Molecular complexes therefore afford a unique opportunity to study and understand the nature of weak intermolecular interactions.[10]

An important method of obtaining mixed crystals is to choose molecules of similar shapes and sizes. Thus, hexachlorobenzene forms solid solutions with a variety of chloro(methyl)benzenes $C_6Cl_x(CH_3)_{6-x}$ $x = 3$, 4, or 5 and also with pentachlorobenzenethiol, and pentachlorophenol (in the latter's disordered high-temperature form).[11] Another recently studied family of compounds where mixed crystals may be obtained is the 2-benzyl-5-benzylidenecyclopentanone group.[12] In all these cases, the forces between molecules are largely isotropic, and this type of behaviour can be considered to be a 'volume effect'. Consequently, solid solutions are formed throughout the composition range. Such mixed crystals have disordered crystal structures, with the amounts of the two constituents depending on the amounts taken originally in solution and on the relative solubilities in the solvent used.

However, it is possible to obtain mixed crystals where the intermolecular forces are strong and highly directional. In these cases, geometric criteria are not the crucial features that determine complex formation. Donor–acceptor complexes are good examples in this category. As is well known, such mixed crystals have fixed stoicheiometries and (usually) ordered structures. So strong and directional are the forces in such complexes that it is often possible to predict crystal packing modes with a high degree of confidence.[13,14]

Between these two extremes, there must remain cases where the interactions between molecules, though stronger and more directional than in the Cl–Me mixed-crystal compounds, are

Table 1. Relative molar amounts[a] of cinnamic acid monomers and cyclobutane dimers at various stages in the solid-state photoirradiation of the complex (**1a**)

Time (h)	% Overall conversion	(**2a**):(**2b**)[b]	(**5a**)	(**5b**)	(**4a**)	(**4b**)	(**4c**)
0	0	2:1	2	1	0	0	0
2	47	2.10:1	1.037	0.555	0.385	0.115	0.193
3	66	1.997:1	0.627	0.404	0.530	0.142	0.314
4	72	2.03:1	0.551	0.287	0.540	0.164	0.371
32(∞)	94	2.09:1	0.150	0.044	0.626	0.164	0.598
—	100[c]	2:1	0	0	0.667[d]	0.166[d]	0.667[d]

[a] As estimated by u.v. spectra of fractions obtained from preparative t.l.c. of methylated, partially reacted solids. [b] The ratio is defined as [(**5a**) + 2(**4a**) + (**4c**)]:[(**5b**) + 2(**4b**) + (**4c**)] and provides a cross-check on the separation and estimation procedures since it should ideally be equal to 2.00:1. [c] A 100% conversion is impossible for this reaction. [d] The values are calculated assuming an ideally disordered structure for the complex (**1a**).

weaker than those in donor–acceptor complexes. Were such complexes to exist, the geometric criteria governing the constituent molecules should neither be as stringent as in the hexachlorobenzene solid solutions nor as incidental as in donor–acceptor crystals, while the degree of order–disorder might be expected to lie between these two limiting cases.

It was felt that Cl ··· Cl interactions belong to this intermediate category since they have been shown to be not only weakly attractive but also somewhat directional in character. Thus, as an extension of the crystal engineering principle, it was sought to co-crystallise various chloro-aromatic compounds so that Cl ··· Cl interactions could be optimised in the crystal. It was felt that, if formed, such mixed crystals of PCAs would afford a more detailed insight into the nature of Cl ··· Cl interactions.

Experimental

The cinnamic acids were prepared by literature methods and satisfactorily characterised. Data collection was carried out at the Regional Sophisticated Instruments Centre, Indian Institute of Technology, Madras. Computation was carried out at the Computer Maintenance Corporation, Hyderabad. The crystal energy calculations were performed with the geometry–energy programm GEO.

6-*Choloro*-3,4-*methylenedioxycinnamic Acid* (**2a**)–2,4-*Dichlorocinnamic Acid* (**2b**) 2:1 *Complex* (**1a**).—The acids (**2a** and **b**) were dissolved in equimolar amounts in a small quantity of EtOH and the solution was carefully evaporated. The complex (**1a**) was obtained as a fine, crystalline solid. Details of physical properties are presented in the Results section, since they have an important bearing on the structure of the complex. The stoicheiometry was inferred from u.v. studies on solutions in MeOH, and the n.m.r. spectrum of a solution in $(CD_3)_2SO$.

Solid-state Irradiation of the Complex (**1a**).—The complex (**1a**) (1 g) was well ground and irradiated with a medium-pressure u.v. lamp for *ca.* 40 h under Pyrex filters. The reaction was monitored by i.r. spectroscopy. The irradiated solid was esterified with CH_2N_2: preparative t.l.c. (silica gel, $CHCl_3$) showed the presence of the three cyclobutane diesters (**4a**—**c**) and the monoesters (**5a** and **b**). The relative amounts of these compounds in this and related experiments were determined by u.v. spectroscopy (MeOH) and are given in Table 1. The diester (**4a**), m.p. 181 °C; $\lambda_{max.}$(MeOH) 295 nm (ε 5 764), was identical with the compound previously reported.[15]

Table 2. Atomic co-ordinates (fractional crystal co-ordinates) for compound (**2a**) (form I)[a,b]

Atom	*X*/*a*	*Y*/*b*	*Z*/*c*
C(1)	0.482 4(21)	0.367 8(7)	−0.244 5(5)
C(2)	0.425 2(24)	0.514 8(7)	−0.197 4(6)
C(3)	0.515 1(22)	0.612 9(7)	−0.250 5(6)
C(4)	0.687 8(23)	0.570 3(8)	−0.345 9(6)
C(5)	0.746 0(24)	0.428 2(8)	−0.396 3(6)
C(6)	0.643 8(20)	0.327 2(7)	−0.341 9(6)
C(7)	0.382 1(23)	0.257 0(8)	−0.191 4(6)
C(8)	0.212 2(24)	0.279 3(8)	−0.102 0(6)
C(9)	0.120 8(22)	0.157 7(8)	−0.059 0(6)
C(10)	0.619 8(32)	0.813 1(9)	−0.304 4(8)
O(1)	−0.044 9(19)	0.196 6(6)	0.0297(4)
O(2)	0.190 1(18)	0.032 1(6)	−0.103 4(5)
O(3)	0.480 8(15)	0.760 6(5)	−0.221 2(4)
O(4)	0.761 8(16)	0.690 7(5)	−0.380 9(4)
Cl	0.725 4(7)	0.146 8(2)	−0.405 5(2)
H(2)	0.280(18)	0.554(6)	−0.128(5)
H(5)	0.900(19)	0.395(6)	−0.495(5)
H(7)	0.454(16)	0.168(6)	−0.234(5)
H(8)	0.108(18)	0.364(6)	−0.061(5)
H(10A)	0.475(25)	0.853(9)	−0.342(7)
H(10B)	0.861(20)	0.864(7)	−0.263(5)
HO	−0.141(43)	0.131(14)	0.065(11)

[a] For labelling of atoms see Figure 1. [b] Estimated standard deviations are given in parentheses.

Dimethyl t-3,t-4-*bis*-(2,4-*dichlorophenyl*)*cyclobutane*-r-1,c-2-*dicarboxylate* (**4b**) was obtained as a white solid, m.p. 108 °C; $\lambda_{max.}$(MeOH) 283 nm (ε 930) (ε_{230} 3 743); $\nu_{max.}$(KBr) 2 960, 1 740, 1 600, 1 580, 1 480, 1 440, 1 200br, 1 100, 1 040, 860, 800, and 780 cm^{-1}; δ($CDCl_3$) 3.76 (s, 6 H), 3.72, 4.82 (q, AA'BB', J_{AB} 7 Hz, 4 H), 7.0 (q, ABX, J_{AB} 9 Hz, 2 H), and 7.24 (d, J_{AX} 1 Hz, 1 H).

Dimethyl 3-(2-*chloro*-4,5-*methylenedioxyphenyl*)-4-(2,4-*dichlorophenyl*)*cyclobutane*-1,2-*dicarboxylate* (**4c**) was obtained as a white crystalline solid, m.p. 76 °C; $\lambda_{max.}$(MeOH) 295 nm (ε 3 570); $\nu_{max.}$(KBr) 2 950, 1 750, 1 600, 1 510, 1 480, 1 440, 1 420, 1 210br, 1 040, and 920 cm^{-1}; δ($CDCl_3$) 3.74, 4.82 (m, 4 H), 3.80 (s, 6 H), 5.96—6.0 (q, 2 H), 6.58 (d, J_{AX} 3 Hz, 1 H), 6.76 (d, J_{XA} 3 Hz, 1 H), 7.06 (q, J_{AB} 8 Hz, 2 H), and 7.24 (d, J_{AX} 1 Hz, 1 H). The n.m.r. spectrum showed a quartet for the $-CH_2O_2-$ group on account of the restricted rotation about the single bond joining the phenyl to the cyclobutane ring. This is good evidence for a β-truxinic structure.[15,16] Variable-temperature studies [$(CD_3)_2SO$] showed that the AB pattern coalesces to give a single sharp line at about 50 °C. The mass spectrum (70 eV) showed ions at *m*/*z* 470(1.5%), 472(1.5), 474(0.5), and 4.76(0.07) (all $M^{+\bullet}$), 326(0.6), 328(0.6), and 330(0.25) (332 not detected) [all $(M - C_6H_8O_4)^{+\bullet}$], 240(100) and 242(34) [both $(C_{11}H_9ClO_4)^{+\bullet}$], 230(10), 232(7), and 234(2) [all $(C_{10}H_8Cl_2O_2)^{+\bullet}$], and 113(47) $(C_5H_5O_3)^+$. The n.m.r. and mass spectra provide complete evidence for the pseudo-mirror-symmetric heterodimer structure.

X-*Ray Structure Determination of* 6-*Chloro*-3,4-*methylenedioxycinnamic Acid* (**2a**), *Form I*.—*Crystal data*: $C_{10}H_7ClO_4$, $M = 226.5$, triclinic, $a = 3.875(3)$, $b = 9.574(6)$, $c = 13.047(6)$ Å, $\alpha = 106.39(4)$, $\beta = 91.97(5)$, $\gamma = 91.30(6)°$, $V = 4.638 \times 10^{-26}$ cm^3, $F(000) = 232$, $\mu = 3.41$ cm^{-1}(Mo-K_α), $D_c = 1.625$ g cm^{-3}, $Z = 2$, space group $P\bar{1}$, confirmed during the refinement, λ(Mo-K_α) = 0.710 87 Å. Unit-cell parameters were determined by a least-squares fit to the settings of 25 accurately centred high-order reflections. Intensity data were collected from a small crystal (0.4 × 0.25 × 0.15 mm) with a computer-controlled Enraf Nonius CAD-4 diffractometer. A total of 761

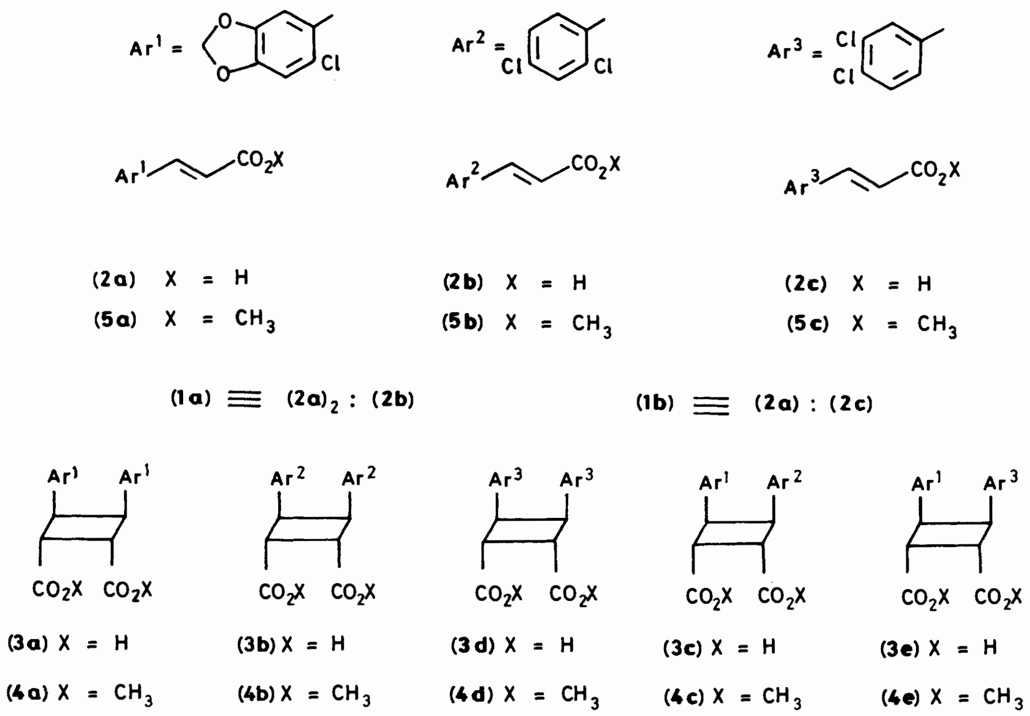

(2a) X = H
(5a) X = CH_3

(2b) X = H
(5b) X = CH_3

(2c) X = H
(5c) X = CH_3

(1a) ≡ **(2a)**$_2$: **(2b)**

(1b) ≡ **(2a)** : **(2c)**

(3a) X = H
(4a) X = CH_3

(3b) X = H
(4b) X = CH_3

(3d) X = H
(4d) X = CH_3

(3c) X = H
(4c) X = CH_3

(3e) X = H
(4e) X = CH_3

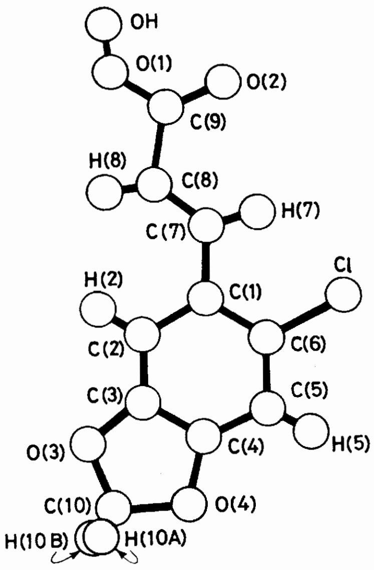

Figure 1. Atom-numbering scheme for the acid **(2a)**

reflections was considered non-zero at the 3σ significance level out of 2 619 possible reflections in the θ range 3—28°. No absorption corrections were applied and there was no evidence for crystal decomposition. The weights were taken as $1.000/\{[\sigma(F_o)]^2 + (0.06F_o)^2\}$ where $\sigma(F_o)$ is the standard deviation based on the counting statistics.

The structure was solved by routine methods using the MULTAN 80 program.[17] Least-squares refinement[18] incorporating positional and anisotropic temperature parameters for the non-hydrogen atoms gave $R = 0.069$. An electron density difference map at this stage revealed the positions of all eight hydrogen atoms including the carboxylic hydrogen atom. When these atoms were incorporated into the refinements with isotropic temperature parameters, a final R value of 0.045 and an R_w value of 0.045 were obtained. Eight reflections of fairly low $\sin\theta/\lambda$ had F_o values that were significantly smaller than F_c and were excluded from the refinements. The final electron density difference map did not reveal any significant electron density above 0.27 e Å^{-3}. The final atomic co-ordinates for **(2a)**, form I are listed in Table 2.* The atom-numbering scheme is given in Figure 1.

Results and Discussion

Formation of Molecular Complexes via Cl · · · Cl *Interactions and their Solid-state Reactivity*.—When 6-chloro-3,4-methylenedioxycinnamic acid **(2a)** and 2,4-dichlorocinnamic acid **(2b)** were dissolved in approximately equimolar quantities in EtOH and the solution was carefully evaporated, white crystals of the 2:1 complex **(1a)** (m.p. 225—226 °C) were invariably the first to crystallise.[19] While the acid **(2b)** has the β-structure[2] and is monoclinic (m.p. 229 °C; $P2_1/c$, $Z = 4$, $a = 3.88$, $b = 6.44$, $c = 36.8$ Å, $\beta = 90.5°$), the acid **(2a)** is dimorphic with both forms triclinic and with the β-structure (form I, $P\bar{1}$, $Z = 2$, $a = 3.875$, $b = 9.574$, $c = 13.047$ Å, $\alpha = 106.39$, $\beta = 91.97$, $\gamma = 91.30°$, $V = 464$ Å^3; form II, $P\bar{1}$, $Z = 2$, $a = 9.05$, $b = 12.94$, $c = 4.10$ Å, $\alpha = 93.3$, $\beta = 95.5$, $\gamma = 74.4°$, $V = 460$ Å^3).[15] A recrystallised sample, m.p. 246 °C, contained both forms. The complex **(1a)** is distinct from both **(2a)** and **(2b)** and from a physical 2:1 mixture of **(2a)** and **(2b)** (m.p. 207—210 °C). Admixture of **(1a)** with either **(2a)** or **(2b)** results in a considerable m.p. depression. When widely different amounts of **(2a)** and **(2b)** are taken into solution, crystals of **(1a)** along with those of the acid in excess (**2a** or **b**) are obtained. *X*-Ray powder traces of **(1a)** and a 2:1 physical mixture of (**2a** and **b**) are reproduced in Figure 2. Crystals of **(1a)** were extremely small, but Weissenberg photographs showed that they were different from those of **(2a)** (both forms) and **(2b)** and, further, revealed a

---

* *Supplementary data* (see section 5.6.3 of Instructions for Authors, in the January issue). Lists of bond lengths and angles and of thermal parameters have been deposited at the Cambridge Crystallographic Data Centre.

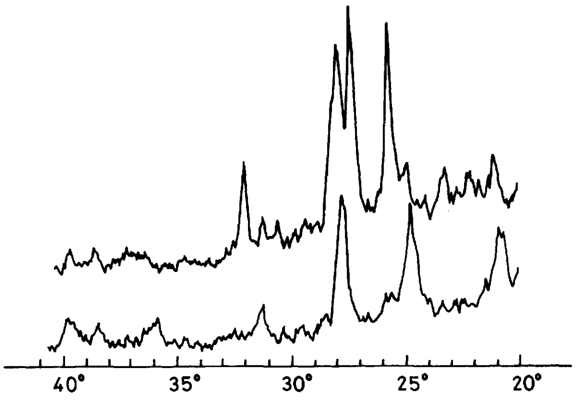

Figure 2. *X*-Ray powder traces (Cu-K_{α_1}) of the complex (**1a**) (bottom) and of a 2:1 mixture of acids (**2a** and **b**) (top). The angle is 2θ

ca. 4 Å short axis and other cell dimensions which bear a resemblance to those of form I of (**2a**) (triclinic, $a = 3.79$ Å, $b^* = 0.1215$, $c^* = 0.1794$, $V = 452$ Å^3). On the basis of all this evidence, we conclude that (**1a**) is a distinct chemical entity, being neither a solid solution nor a mixture of (**2a** and **b**).

In a set of related experiments, the co-crystallisation of the acid (**2a**) and 3,4-dichlorocinnamic acid (**2c**) was studied. The acid (**2c**) has been reported as having the β-structure with the 'crystals very poorly developed'.[2] We have found, however, that this acid is also dimorphic and yields good crystals from EtOH. Both forms are monoclinic and, as expected, have the β-structure (needles, $P2_1/c$, $Z = 4$, $a = 3.9$, $b = 6.56$, $c = 36.84$ Å, $\beta = 91.5°$, $V = 942$ Å^3; plates, $P2_1/c$, $Z = 4$, $a = 14.2$, $b = 3.92$, $c = 17.0$ Å, $\beta = 92°$, $V = 946$ Å^3). The crystallised sample contains both forms. When acids (**2a** and **c**) are taken together in EtOH, a variety of solids are obtained, in contrast to the behaviour of the (**2a**)–(**2b**) combination already described. We have, on various occasions, obtained the 1:1 complex (**1b**), m.p. 217—218 °C, and solids with a wide (5—25 °C) melting range and with compositions between 7:1 and 1:3 of (**2a**) and (**2c**), respectively.[20]

As expected, pure (**2a**), (**2b**), and (**2c**) yield the respective topochemical β-truxinic acids on irradiation >300 nm. However, when crystals of (**1a**) were irradiated under similar conditions and the resulting solid was methylated, all three cyclobutane diesters (**4a**—**c**) were found in addition to the monoesters (**5a**) and (**5b**). Similarly, when solid (**1b**) was irradiated and the product worked up as before, a mixture of diesters (**4a**, **d** and **e**) and monoesters (**5a** and **c**) was obtained.

Crystal Structures of the Two Forms of the Acid (**2a**) *and the Structures of the Complexes* (**1a** *and* **b**).—The formation of all three mirror- or pseudo-mirror-symmetry cyclobutanes (**3a**—**c**) shows that, in the solid complex (**1a**), (**2a** and **b**) are related by a 4 Å stack translation, with all three types of contacts [(**2a**)–(**2a**), (**2b**)–(**2b**), and (**2a**)–(**2b**)] possible. Similarly, the product distribution from (**1b**) shows that potentially reactive (**2a**)–(**2a**), (**2c**)–(**2c**), and (**2a**)–(**2c**) groupings are present in this latter complex.

Clearly, a short axis of 3.88 Å for (**1a**) shows that there is a random occupation of crystallographic sites in the stack direction by (**2a**) and (**2b**) molecules. In accordance with this, the relative amounts of the three cyclobutanes (**3a**—**c**) at maximum conversion are very close to the theoretically expected 4:1:4 ratio for a statistical *2:1* distribution of acids (**2a** and **b**) along the stack (Table 1). Likewise, the cyclobutanes (**3a**, **d** and **e**) are formed in 1:1:2 ratio from the complex (**1b**), indicating a random 1:1 distribution of acids (**2a** and **c**) in the stack direction. Equal amounts of (**3a**) and (**3c**) from (**1a**) can be rationalised by a variety of models but the formation of (**3b**) and the 4 Å axis are difficult to explain unless (**2a**) and (**2b**) are disordered in (**1a**).

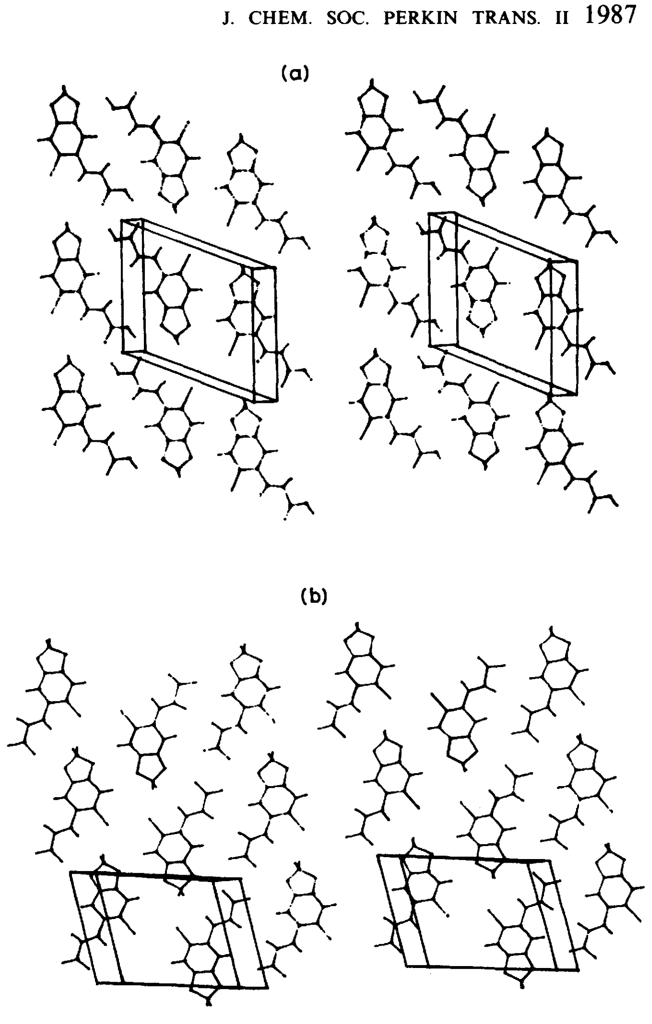

Figure 3. (*a*) Stereoview of the crystal structure (solved) of the acid (**2a**) (form I); (*b*) stereoview of the crystal structure (computed) of the acid (**2a**) (form II)

The crystal quality of (**1a**) was extremely poor [the complex (**1b**) did not form recognisable crystals] and did not permit the collection of counter data. However, it was surmised that the structure of (**1a**) could be rationalised by a model where the minor component (**2b**) has been induced to co-crystallise in the crystal structure of the major component (**2a**). The main reasons for this assumption are as follows. (*a*) The acid (**2a**) is the major constituent of the complex (**1a**). (*b*) The cell dimensions of (**1a**) are similar to those of (**2a**) (both forms), whereas (**2b**) belongs to a different crystal system. (*c*) The acid (**2a**) forms a 1:1 complex with the related acid (**2c**) which is isomeric with (**2b**), yet (**2b**) and (**2c**) do not form complexes with each other.

Accordingly, the knowledge of the crystal structures of the two forms of (**2a**) was deemed crucial for any understanding of the structure of (**1a**) and of any possible role of Cl···Cl interactions in the stabilisation of such a complex.

The crystal structure of the all-obtuse form I of (**2a**) was solved by direct methods from counter data and refined satisfactorily to an *R* value of 0.045. Table 2 is a list of atomic positional parameters. Figure 3(*a*) is a stereoview of the structure looking down the short axis. The cell parameters of the all-acute form II are closely related to those of form I and to those of the non-chloro analogue (**6**) ($P\bar{1}$, $Z = 2$, $a = 3.804$, $b = 10.502$, $c = 11.112$ Å, $\alpha = 77.84$, $\beta = 84.26$, $\gamma = 80.17°$), the crystal structure of which is known.[15] This information was employed to obtain a possible structure for form II using packing calculations with atom–atom potentials.[21] The reason

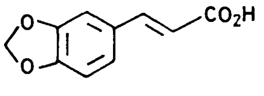

(6)

for adopting this approach was because the form II crystals were obtained as slender needles, unsuitable for data collection. Figure 3(*b*), which is a stereoview of the calculated form II structure projected down the short axis, shows that the two structures are closely related.

The projection of molecules in Figure 3(a) is in the form of a molecular sheet in which acid molecules form inversion-related hydrogen-bonded dimers. Surprisingly the only intra-sheet Cl $\cdots$ Cl contact is as long as 3.90 Å. However, there are short intra-sheet C–H $\cdots$ O contacts of 2.44 and 2.58 Å. The latter have been referred to as 'hydrogen bonds' and are discussed in greater detail in the following paper.[22] Such bonds have been described by Taylor and Kennard as being not only weakly attractive in nature but also quite directional in character.[23] Thus they are similar to Cl $\cdots$ Cl interactions and it is no surprise that both type of interactions are involved in establishing a sheet structure. There are also hints of very weak C–H $\cdots$ Cl interactions of 3.28 Å which may be sheet-stabilising. All in all, the sheet structure in the form I crystal of (**2a**) is very reminiscent of the molecular sheet in triclinic hexachlorobenzene and the structures of these two β-crystals are built up in exactly the same manner, by van der Waals stacking of sheets to generate the 4 Å short axis. Form II of (**2a**) also has a sheet structure and Figure 3(b) shows that the sheet is characterised by the same interactions as in form I. The notable features in forms I and II are (*a*) intra-sheet O–H $\cdots$ O hydrogen bonding; (*b*) intra-sheet Cl $\cdots$ Cl, C–H $\cdots$ O, and C–H $\cdots$ Cl interactions; and (*c*) inter-sheet C $\cdots$ C (and to some extent C $\cdots$ Cl and Cl $\cdots$ Cl) interactions. It is quite possible that C–H $\cdots$ O contacts are of greater importance than Cl $\cdots$ Cl contacts in sheet stabilisation of both forms of the acid (**2a**).

The structures of (**1a** and **b**) may now be considered. The acids (**2a**—**c**) are chemically, geometrically, and structurally similar; they occupy volumes of 232, 230, and 235 A^3 in their native structures. All adopt the β-structure. The molecular shapes, though similar, are not identical (Figure 4). Complex formation, especially in (**1a**), between molecules of slightly differing shapes and volumes, and the fixed stoicheiometries in (**1a** and **b**) are indications that directional Cl $\cdots$ Cl, C–H $\cdots$ O, and C–H $\cdots$ Cl forces are involved.

The incorporation of (**2b**) or (**2c**) molecules in a fixed ratio of 1:2 (or 1:1) but in a disordered stack fashion in the sheet-based crystal structure of (**2a**) may be modelled according to any of the following possibilities.

(*a*) The acids (**2a** and **b**) are disordered over all sites within a 2:1 ratio. The stacking is necessarily disordered and would explain the solid-state products and their distribution.

(*b*) A particular sheet contains either (**2a**) or (**2b**) molecules but there are twice as many sheets of (**2a**) as of (**2b**) and both types of sheet are stacked in a disordered fashion.

(*c*) Each sheet has an ordered structure with 2:1 stoicheiometry, but the sheets are stacked randomly.

Similar arguments would apply for the complex (**1b**).

A complete scrambling of (**2a** and **b**) over all crystallographically identical sites [possibility (*a*)] is tantamount to intra-sheet solid-solution behaviour. Since only the 2:1 complex is obtained from (**2a**) and (**2b**), this model is untenable.

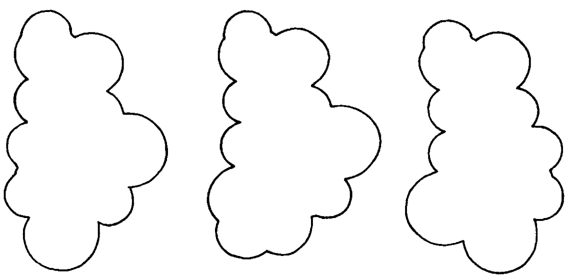

(2b) **(2a)** **(2c)**

Figure 4. Cross-sectional areas of the molecules (**2a**—**c**)

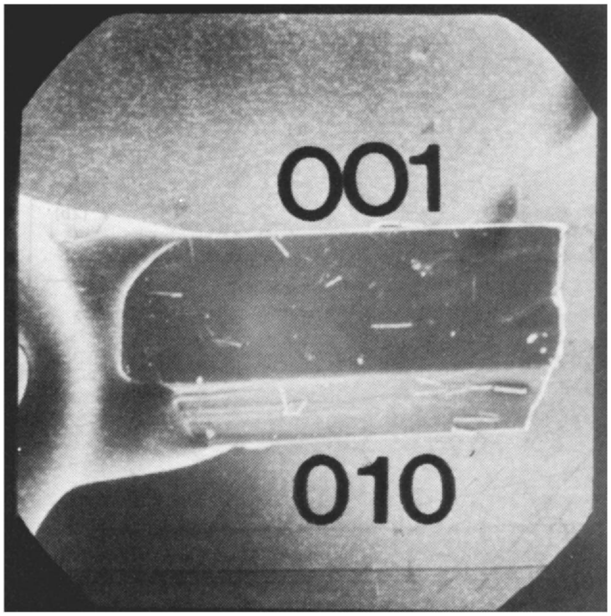

Figure 5. Scanning micrograph (× 758) of a single crystal of the acid (**2a**); the needle direction is [100] and faces (010) and (001) may be seen

Possibility (*b*) is also not in keeping with the known facts. While both (**2a**) and (**2b**) may form molecular sheets there is little reason why twice as many sheets of (**2a**) should be formed. The only conceivable means of this occurring is if each sheet (**2a** or **b**) 'recognises' the next one in the stack in a very specific way. However, this would imply a degree of order in the stack direction which is not observed, given the solid-state reaction products and their distribution.

In possibility (*c*) the stacking is presumed disordered. This may be understood easily since the major stacking interactions are the C $\cdots$ C and C $\cdots$ Cl ones which are not particularly specific for (**2a** or **b**). If this were the case, one would conclude that the sheets should be ordered and most probably because Cl $\cdots$ Cl, C–H $\cdots$ O, and other sheet-stabilising interactions which are optimised in the sheet plane are directionally specific and can discriminate between acids (**2a** and **b**). Further, any mechanism for such sheet-ordering must explain the particular stoicheiometries obtained and the fact that the (**2a**)—(**2c**) combination in solution is prone to result in the crystallisation of not only the complex (**1b**) but also a series of solid solutions and mixtures of (**2a** and **c**).

In view of the assumed similarity between the crystal structures of (**1a**) and (**2a**), we have attempted to model the crystallisation of (**1a**) by the adsorption of (**2a** and **b**) molecules on the growing faces of an embryonic (**2a**) template crystal. Figure 5 gives the morphology of a form I crystal of (**2a**). The needle

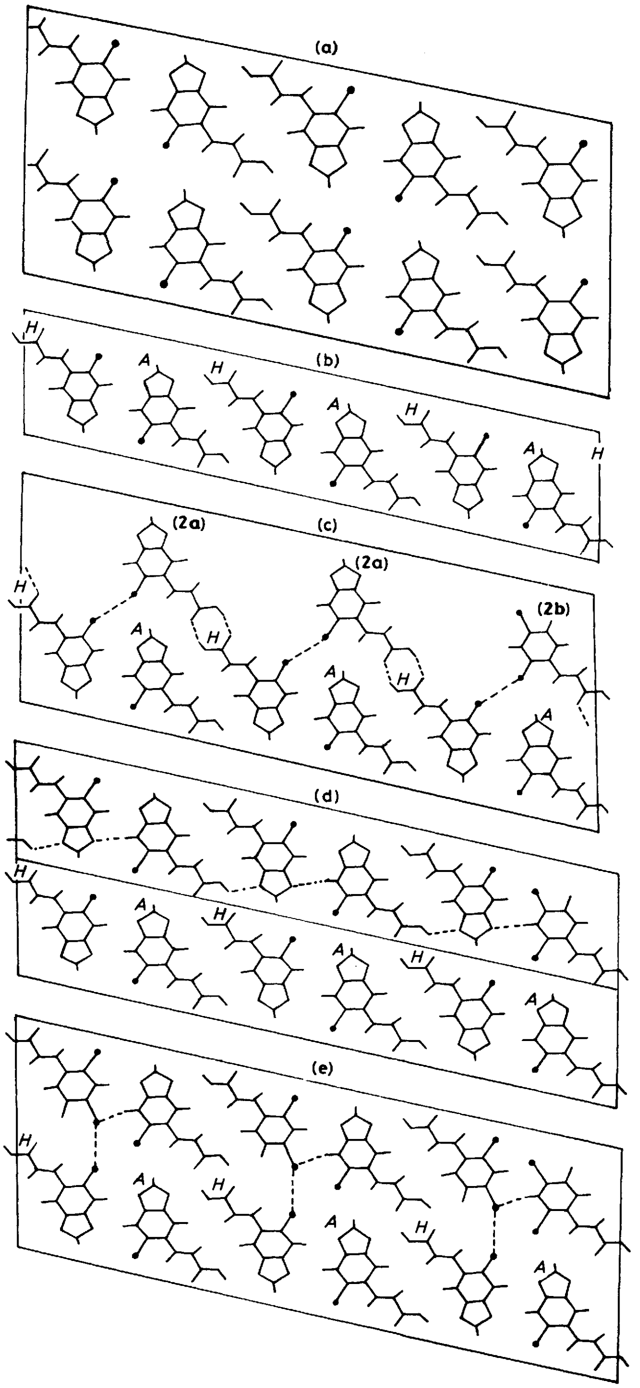

Figure 6. (*a*) Disposition of intra-sheet (**2a**) molecules along the (010) and (001) faces of the form I crystal; Cl atoms are shaded. (*b*) *A* and *H* sites on the (010) face. (*c*) Crystallisation of (**2a**) and (**2b**) molecules at the *H* sites by means of carboxylic hydrogen bonding. Note that both kinds of molecules may be attached with almost equal ease. (*d*) Attachment of (**2a**) molecules at the *A* sites so that O–H ··· O(C)$_2$ and C–H ··· O bonding is optimised. (*e*) Attachment of (**2b**) molecules at the *A* sites. Note that this situation appears less favourable than that depicted in Figure 6(*d*)

direction is along [100] and represents the stacking of molecular sheets. The growth of an individual sheet, however, is along the (001) and (010) faces. The arrangement of molecules along these faces is shown in Figure 6(*a*). Growth on (010) is much faster than on (001) and the intra-sheet crystallisation of (**1a**) is expected to be largely governed by the relative ease with which (**2a** and **b**) molecules are able to crystallise on the growing (010) face and to some extent on the (001) face. Similar arguments could be invoked for the form II crystal, but owing to the similarity of both forms, the following discussion will be restricted to form I.

Figure 6(*b*) shows molecules on the (010) face in the form I nucleus crystal. While every alternate molecule presents its carboxylic end towards this face, the centrosymmetric counterparts have their methylenedioxy aromatic group pointing towards the same face. Growth parallel to (010) involves then the adsorption of molecules at two distinct sites which will be referred to as the hydrogen-bonded (*H*) and aromatic (*A*) sites. From a solution containing both (**2a** and **b**) molecules, either molecule may be attached at the *H* sites since O–H ··· O bonding is involved in either case. These possibilities are condensed in Figure 6(*c*) from which it may be noted that these newly attached hydrogen-bonded molecules are also held to the crystal through Cl ··· Cl contacts of *ca.* 3.9 Å. These contacts involve the *ortho*-Cl group and are therefore possible for both (**2a**) and (**2b**) molecules. So for half the sites on (010), there is an equal (or almost equal) probability that (**2a** or **b**) may substitute for (**2a**) molecules.

The crystallisation of molecules in the interleaving *A* sites may be considered next. The interactions which link molecules at the *A* sites are of the C–H ··· O, O–H ··· O(C)$_2$, Cl ··· Cl and C–H ··· Cl types. Although weaker than carboxylic acid hydrogen bonds, these interactions are able to discriminate between (**2a**) and (**2b**) molecules. While the (**2a**) molecule is held in place by two fairly specific C–H ··· O and C–H ··· O(C$_2$) bonds involving the heterocyclic oxygen atoms, the (**2b**) molecule, if inserted, must be stabilised with only one Cl ··· Cl and possibly one weak C–H ··· Cl contact *in lieu* of the foregoing interactions [Figures 6(*d*) and (*e*)]. Owing to the different shapes of the (**2a**) and (**2b**) molecules, especially in the region of the 3- and 4-positions of the aromatic ring (Figure 4), the (**2a**) molecule fits much better at the *A* site than the (**2b**) molecule. By very similar arguments, details of which have been presented elsewhere,[24] it may be shown that when the next row of molecules is attached, the alternate registry of ordered and disordered sites is expected to be maintained.

If the *H* sites may be occupied by (**2a**) or (**2b**) with equal probability while only (**2e**) molecules occupy the *A* sites, a sheet stoicheiometry of 3:1 (**2a**):(**2b**) would appear to result. Sheet growth, however, occurs along both (010) and (001) and the overall sheet stoicheiometry is the result of competitive crystallisation of (**2a** and **b**) molecules at both these faces. It may be shown that sheet growth on (010) and (001) simultaneously should result in a stoicheiometry between 3:1 and 1:1, and so the overall (**2a**):(**2b**) ratio could be close to 2:1.

The 1:1 stoicheiometry of (**2a**) and (**2c**) in the complex (**1b**) can also be understood with this model for mixed crystallisation. Since (**2a** and **c**) molecules resemble each other in shape much more closely than (**2a** and **b**), each acid may mimic the behaviour of the other and enter either the *H* or the *A* sites with about the same ease. The behaviour is more of the solid-solution type, as has been observed experimentally.

This disorder mechanism for the formation of the complex (**1a**) is supported by the experimentally observed stoicheiometries for different samples of the complex. These values vary slightly (1:2.03; 1:2.05; 1:2.08). The differences are around the error limit (5%) but the very fact that (**1a**) is obtained unfailingly from (**2a** and **b**) (instead of mixtures) suggests that the forces between molecules are directionally specific. So if the growth is along the same faces, rather similar stoicheiometries should be obtained. The simple 2:1 stoicheiometry does not seem to be a fortuitous average over many growth faces but occurs because the acid (**2a**) crystals (Figure 5) are bounded by very few faces where two growth sites *A* and *H* can discriminate effectively between (**2a** and **b**) molecules. The situation is somewhat different for (**1b**) and related solids. Much wider variations in the (**2a**):(**2c**) ratio are obtained. Whether these solids should be referred to as structural variations of (**1b**) or whether (**1b**) is part of a structural continuum is a moot point. However, all this hints at a disordered structure.[20]

It is noteworthy that seemingly minor geometrical differences in (**2b** and **c**) can result in a considerable amplification of the structural differences between complexes (**1a**) and (**1b**). Weak but non-trivial Cl ··· Cl and other forces may discriminate between these subtle shape differences in (**2b** and **c**) and include molecules of the 'right' shape or substitutional pattern with a high degree of selectivity in a manner reminiscent of enzyme action.

Kinetics of the Solid-state Reactions which occur on Irradiation of the Complex (**1a**).—The complex (**1a**) is also of interest from the point of view of comparing the relative rates of solid-state reactions. The kinetics of topochemical processes, though of fundamental mechanistic interest, have not been studied in detail since it is inherently difficult to compare reactions which occur in different crystals. Factors such as preparation history and defect profiles normally preclude direct comparisons of reaction rates from sample to sample. Further, these rates may depend greatly on supposedly innocuous experimental conditions. For instance, the rates of topochemical dimerisation of the acid (**2c**) have been found to depend substantially on whether the solid material is suspended in water or in hexane during irradiation.[25] Another complication, at least for the β-type crystals, is that the maximum expected theoretical yield is less than 100%. It has been shown[26] that for an ideal β-crystal this maximum theoretical yield is about 85%, with experimental deviations from this value being large; yields as low as 30% and as high as 90% have been reported for various β-cinnamic acids.[1] Such deviations reflect intrinsic differences in reaction rates but these are difficult to quantify.

Several of these problems may, however, be circumvented if the various reactions which one attempts to compare occur within the same crystal, and the complexes (**1a** and **b**) probably represent the first cases among organic photoreactive solids where several chemically dissimilar reaction sites have been created through the device of crystal engineering. Since dimers (**3a**—**c**) are all produced in the same crystal, their relative rates of formation are a measure of intrinsic solid-state reactivity differences. Inspection of Table 1 shows that these rates are, in decreasing order, (**3b**) > (**3a**) > (**3c**).

A possible reason for these differences in rates and in the maximum yields could be because the stack spacings are slightly different. While most β-cinnamic acids with short axis between 3.85 and 4.15 Å are known to react upon u.v. irradiation, any such reaction will be accompanied by a reduction in the distance between reacting molecules from *ca.* 4 to *ca.* 1.6 Å. This reduction must result in a concomitant relaxation of the neighbouring unchanged molecules so that the 'new' distance between incipient reactive molecules is now greater than the short axis. For crystals with short axis of 4.0 Å or less, such a relaxation probably does not affect photoreactivity. However, if the short axis is greater than 4.0 Å, as for example in form II of the acid (**2a**) (4.10 Å), molecular relaxation that follows initial reaction could place molecules beyond the photoreactive threshold. This may explain why the rate of photoreaction of the acid (**2a**) falls off after an initial period and the maximum yield is only 70%, whereas the acid (**2b**) (short axis 3.88 Å) is converted much more rapidly into dimer in 90% overall yield. In the context of the complex (**1a**), however, it is difficult to decide whether the three distinct molecular pairs have different stack spacings or not.

Further, it is not very clear why the pseudo-mirror-symmetric heterodimer (**3c**) is formed at a rate significantly less than that for either (**3a**) or (**3b**). Table 1 shows that after 4 h, while the maximum possible amount of (**3b**) and 90% of the final amount of (**3a**) have been produced, only about 60% of the final amount of (**3c**) has been produced. So, while the early stages of the reaction mostly involve symmetrical dimer formation, heterodimer formation is the significant process in the later stages. Similar behaviour has been observed for solid solutions of substituted stilbenes and cinnamamides.[27]

Acknowledgements

We thank Professor S. Subramanian who arranged for diffractometer time at I.I.T., Madras, and Professor L. Leiserowitz for the suggestion that the fixed stoicheiometries of the complexes reported here might be due to selective adsorption of the constitutents from solution. The program GEO was generously supplied by Dr. S. K. Kearsley. Financial assistance from the D.S.T. (S.E.R.C.) and from the U.G.C. (Special Assistance Programme) is gratefully acknowledged.

References

1 M. D. Cohen, G. M. J. Schmidt, and F. I. Sonntag, *J. Chem. Soc.*, 1964, 2000.
2 G. M. J. Schmidt, *J. Chem. Soc.*, 1964, 2014.
3 G. M. J. Schmidt, *Pure Appl. Chem.*, 1971, **27**, 647.
4 J. M. Thomas, *Philos. Trans. R. Soc. London, Ser. A*, 1974, **277**, 251.
5 G. R. Desiraju, *Endeavour*, 1984, **8**, 201.
6 K. Mirsky and M. D. Cohen, *Chem. Phys.*, 1978, **28**, 193.
7 D. E. Williams, *Chem. Phys.*, 1981, **55**, 163.
8 J. A. R. P. Sarma and G. R. Desiraju, *Chem. Phys. Lett.*, 1985, **117**, 160.
9 G. R. Desiraju, *Proc. Indian Acad. Sci.* (*Chem. Sci.*), 1984, **93**, 407.
10 A. I. Kitaigorodskii, 'Mixed Crystals,' Springer Verlag, Berlin and Heidelberg, 1984.
11 G. R. Desiraju and J. A. R. P. Sarma, *Proc. Indian Acad. Sci.* (*Chem. Sci.*), 1986, **96**, 599; M. A. Masood and G. R. Desiraju, *Chem. Phys. Lett.*, 1986, **130**, 199.
12 W. Jones, C. R. Theocharis, J. M. Thomas, and G. R. Desiraju, *J. Chem. Soc., Chem. Commun.*, 1983, 1443.
13 G. R. Desiraju and J. A. R. P. Sarma, *J. Chem. Soc., Chem. Commun.*, 1983, 45.
14 J. A. R. P. Sarma and G. R. Desiraju, *J. Chem. Soc., Perkin Trans. 2*, 1985, 1905.
15 G. R. Desiraju, R. Kamala, B. H. Kumari, and J. A. R. P. Sarma, *J. Chem. Soc., Perkin Trans. 2*, 1984, 181.
16 J. A. R. P. Sarma and G. R. Desiraju, *Indian J. Chem., Sect. B*, 1984, **23**, 658.
17 G. Germain, P. Main, and M. M. Woolfson, *Acta Crystallogr., Sect. A*, 1971, **27**, 368.
18 G. M. Sheldrick, SHELX-76; $R = \Sigma||F_o| - |F_c||/\Sigma|F_o|$; $R_w = [\Sigma w||F_o| - |F_c||^2/\Sigma w|F_o|^2]^{1/2}$.
19 J. A. R. P. Sarma and G. R. Desiraju, *J. Chem. Soc., Chem. Commun.*, 1984, 145.
20 J. A. R. P. Sarma and G. R. Desiraju, *J. Am. Chem. Soc.*, 1986, **108**, 2791.
21 S. K. Kearsley and G. R. Desiraju, unpublished work.
22 J. A. R. P. Sarma and G. R. Desiraju, following paper.
23 R. Taylor and O. Kennard, *J. Am. Chem. Soc.*, 1982, **104**, 5063.
24 J. A. R. P. Sarma, Ph.D. Thesis, University of Hyderabad, 1986.
25 F. Nakanishi, H. Nakanishi, M. Tsuchiya, and M. Hasegawa, *Bull. Chem. Soc. Jpn.*, 1976, **49**, 3096.
26 G. R. Desiraju and V. Kannan, *Proc. Indian Acad. Sci.* (*Chem. Sci.*), 1986, **96**, 351, and references cited therein.
27 M. D. Cohen and R. Cohen, *J. Chem. Soc., Perkin Trans. 2*, 1976, 1731.

Received 20*th June* 1986; *Paper* 6/1251